2.0 Methodology

2.1 Analysis Technique

A computer program was written to better model the heat transfer taking place within the H2 air cooler. The program, written in C++, calculates the heat transfer from the air to the cooling water on a row-by-row basis using convective relations for the air and water interfaces and conduction equations for the tube walls. The cooler inlet state is given for air and water, as well as the cooler geometry and material properties. The flowchart in figure 6 shows an overview of the program functionality.

The calculations that take place within the main calculation loop (labeled "Solve Row_j" in the flowchart), are presented by figure 7. For each row, the thermodynamic properties of air and water are computed based on the inlet states. For the initial tube row, the cooler inlet properties are used. For successive downstream tube rows, the outlet state of the previous tube row is initialized as the inputs for the current row of interest.

In order to first begin a higher fidelity model, a better evaluation of air properties must be used. For this purpose, a function was developed to calculate real gas properties for equilibrium air at temperatures between 0-30,000 K (0-54,000°R) and pressures between 10^{-4}-100 atm based on the curve fit data from Gupta, et al. in reference [4]. The thermodynamic properties calculated by these equations represent a three dimensional surface with temperature and pressure as the abscissae and the relevant thermodynamic property as the ordinate.

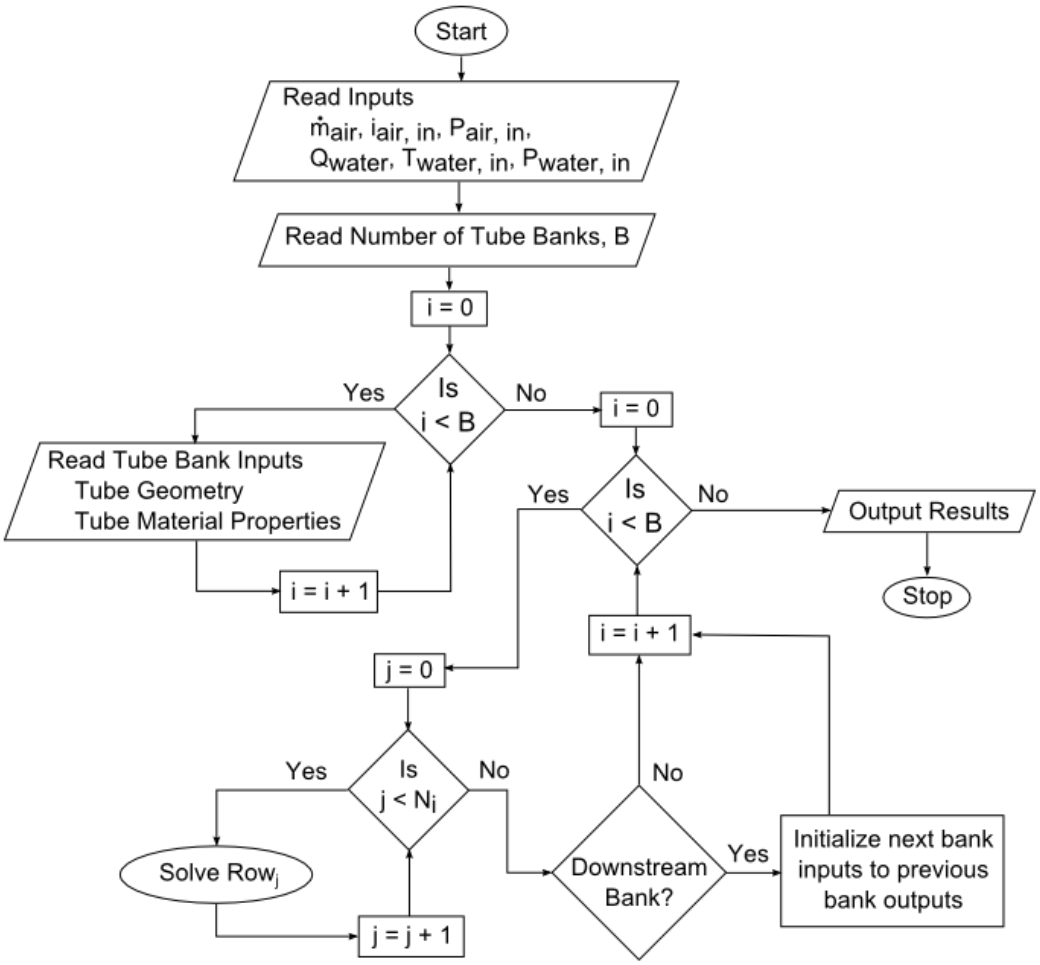

Figure 6 - Program Overview Flowchart

Because total enthalpy is given as the program input, an iterative loop is used to converge on the inlet air temperature for the given inlet pressure by minimizing the residual error in the enthalpy calculation. Once the temperature is calculated, the remaining thermodynamic properties are calculated using their respective surface fit equations, the calculated temperature, and the input pressure. This operation is notionally shown in the flowchart given in figure 8. Similarly, the thermodynamic properties of water are computed by data given by

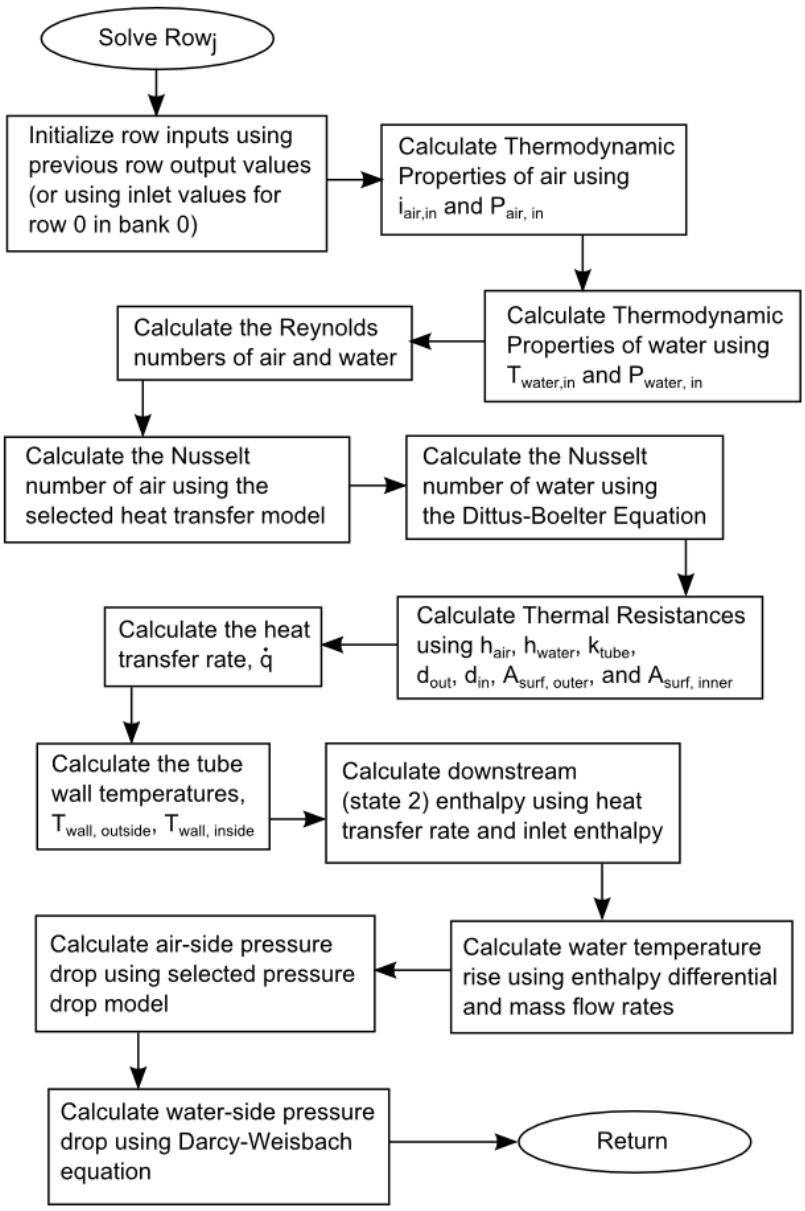

Figure 7 - Row Solver Algorithm Overview Flowchart

the International Association for the Properties of Water and Steam (IAPWS) in references [5] and [6].

The program compares four different heat transfer correlations to determine which has the smallest residual error when compared to the measured data. The heat transfer correlations are used to compute the Nusselt number characterizing

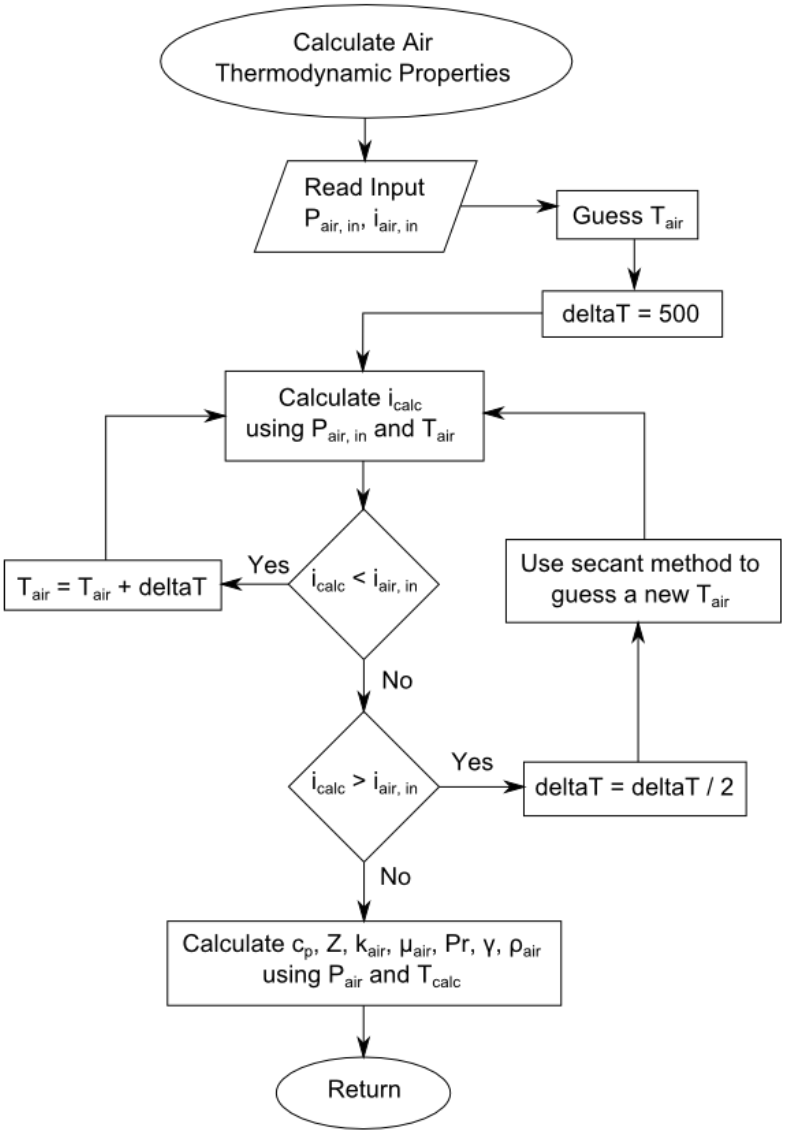

Figure 8 - Air Thermodynamic Properties Solver Overview

the convective strength of the flow. This is used to calculate the heat transfer from the air to the cooling water using the first law of thermodynamics. Then the water temperature rise is cumulatively fed forward through the discretized heat exchanger equations.

The program also compares several different pressure drop models to determine which relationship gives the best match to the measured data. For

completeness, the Darcy-Weisbach pressure drop equation is used to model the water-side pressure drop; though this varies the thermodynamic properties little.

2.2 Heat Transfer Models

Traditional empirical methods for heat exchanger analysis typically specify a lower bound Prandtl number of 0.7 and a lower bound Reynolds number of 2000. For the inlet conditions of the H2 cooler, the temperatures are high enough that the air may have a Prandtl number around 0.55 and the Reynolds number may be less than 150. These input conditions must be acceptable for the heat transfer models used by the program.

When evaluating the heat transfer from the air to the cooling water, the efficacy of the energy exchange is typically a function of the Reynolds number of the flow, the Prandtl number of the flow, and a coefficient that is empirically

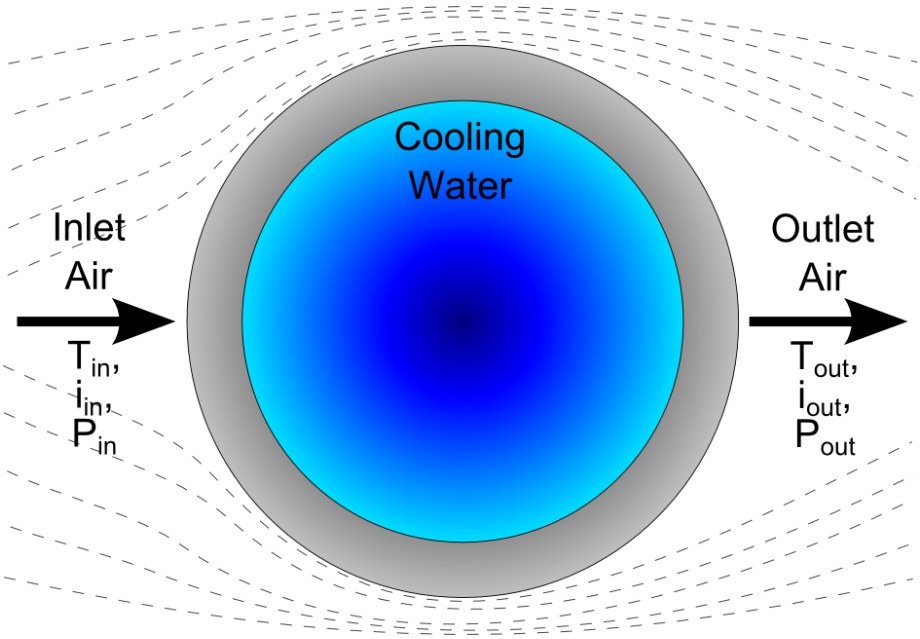

Figure 9 - Single Tube Control Volume

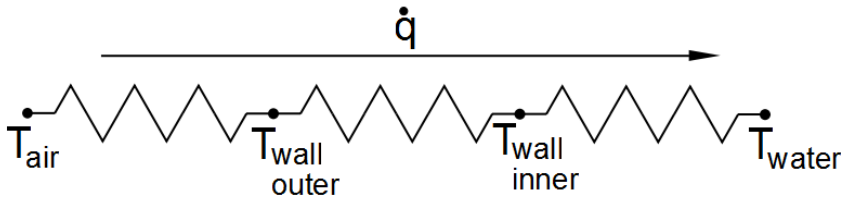

Figure 10 - Equivalent Resistance Circuit Analogy

determined based on the heat exchanger geometry and tube arrangement. These factors are used to evaluate the Nusselt number, Nu, and is typically expressed by a similarity equation of the form[8][9]:

$$Nu \propto \varphi(Re)^m(Pr)^n \quad \text{where } \varphi \text{ is a generic scalar variable} \tag{1}$$

The Nusselt number is used to calculate the convective heat transfer coefficient (h) which is used to quantify the heat energy transferred from the air to the tube wall ($\dot{q}$).

Before it is possible to quantify the amount of heat transfer through the system, the control volume of interest must be defined and the analytic models for the calculation must be developed. Consider the control volume around a single tube as shown in figure 9. This control volume has elements of internal flow convection (the cooling water), external flow convection (cross flow of air over a body), and conduction heat transfer (through the tube wall).

It may be observed that the system may be modeled by use of a circuit analogy as applied to the heat transfer relations as shown in figure 10. By this analogy, the heat transfer may be computed directly using the known inlet air and water temperatures and a calculated equivalent thermal resistance using equation 2 below.

$$\dot{q} = \frac{T_{air} - T_{water}}{R_{eq}} \tag{2}$$

From the first law of thermodynamics, equation 2 can be expressed as:

$$\dot{q} = \frac{T_{air} - T_{water}}{R_{eq}} = \dot{m}_{air}\Delta i = \dot{m}_{air}(i_{in} - i_{out}) \tag{3}$$

where i_{in} is the inlet air enthalpy and i_{out} is the outlet air enthalpy as shown for the single tube control volume in figure 9.

The equivalent thermal resistance of this system is given as the sum of the individual resistances—these being the air-side convection term, the tube wall conduction term, and the water-side convection term.

$$R_{eq} = R_{air} + R_{wall} + R_{water} \tag{4}$$

The water-side thermal resistance is calculated based on the result of the Dittus-Boelter equation[7] for internal flow:

$$Nu = 0.023(Re)^{4/5}(Pr)^{n} \tag{5}$$

Where: $n = 0.4$ (for heating)

$n = 0.3$ (for cooling)

The operation of the heat exchanger is such that the air temperature is greater than the water temperature; thus, from an internal flow perspective, the cooling water will be heated and the exponent $n = 0.4$ is used.

From equation 5, the convective coefficient was evaluated as:

$$h_{water} = \frac{(Nu)\, k_{water}}{d_{in}} = \frac{0.023\ (Re)^{0.8}(Pr)^{0.4} k_{water}}{d_{in}} \tag{6}$$

The results of equation 6 were used to evaluate the water-side thermal resistance as:

$$R_{water} = \frac{1}{h_{water} A_{surf,i}} \tag{7}$$

Now, the tube wall thermal resistance must be evaluated. This is done by recognizing that the conduction equation in cylindrical coordinates is given by

$$\dot{q} = -kA\frac{dT}{dr} = -k(2\pi rL)\frac{dT}{dr} \tag{8}$$

For a hollow cylinder, this becomes[7]:

$$\dot{q} = \frac{2\pi Lk\left(T_{s,1} - T_{s,2}\right)}{\ln\left(\frac{r_2}{r_1}\right)} \tag{9}$$

Based on equation 9, it can be seen that the thermal resistance for a hollow cylinder is given by:

$$R_{wall} = \frac{\ln\left(\frac{d_{out}}{d_{in}}\right)}{2\pi k_{wall} L} \tag{10}$$

The air-side thermal resistance is of significant interest. The cross-flow environment in this particular application is such that the conditions are outside of the bounds of traditional heat transfer models. The air-side thermal resistance

follows the form of equation 11 for smooth-tubes with a modification for finned tubes to account for the increased surface area as shown in equation 11a. A derivation of equation 11a may be found in Appendix A.

$$R_{air} = \frac{1}{h_{air} A_{surf,o}} \tag{11}$$

$$\left(\text{for finned tubes}^{[7]}\right) \quad R_{air} = \frac{1}{h_{air} A_T \left[1 - \frac{N_f A_f}{A_T}\left(1 - \eta_f\right)\right]} \tag{11a}$$

Similar to equation 6, the air-side convective heat transfer coefficient is evaluated as:

$$h_{air} = \frac{(Nu)\, k_{air}}{d_{out}} \tag{12}$$

The air-side convective heat transfer coefficient cannot be determined without first calculating the Nusselt number. As mentioned previously, this calculation will be of the form given by equation 1 with variations to account for bank geometries.

Note that the equations presented thus far were developed from the perspective of flow over a single tube. The number of tubes per row (N_T) must be taken into account to determine the total heat transfer through that tube row.

For the scope of this paper, only the heat transfer relations for a staggered array of tubes is examined; though, in practice, in-line arrays of tubes may be found in many applications. Heat transfer from banks of tubes depends on the flow conditions, tube geometries, and tube arrangements. Regarding the flow

conditions, the heat transfer from the shell-side fluid to a tube in the first row of the bank differs from that of a single tube due to the influence of other tubes within that row as well as any tubes in the transverse and diagonal planes.[7] It is for this reason that all four models presented have a correction for the number of tubes in the heat exchanger. This correction is to account for the front-row tube being coated by a relatively smooth boundary layer formed by an undisturbed freestream; however, successive downstream tubes benefit from augmented heat transfer due to the eddies of the turbulent wake created by upstream tubes[11]. It should be noted that a traditional critical transitional numbers for a turbulent wake of a cylindrical body in crossflow occur at $Re \sim 40$[11]. Since the heat transfer relations are based on empirical data, turbulent phenomena (such as vortex shedding) are thought to be included in the correlations.

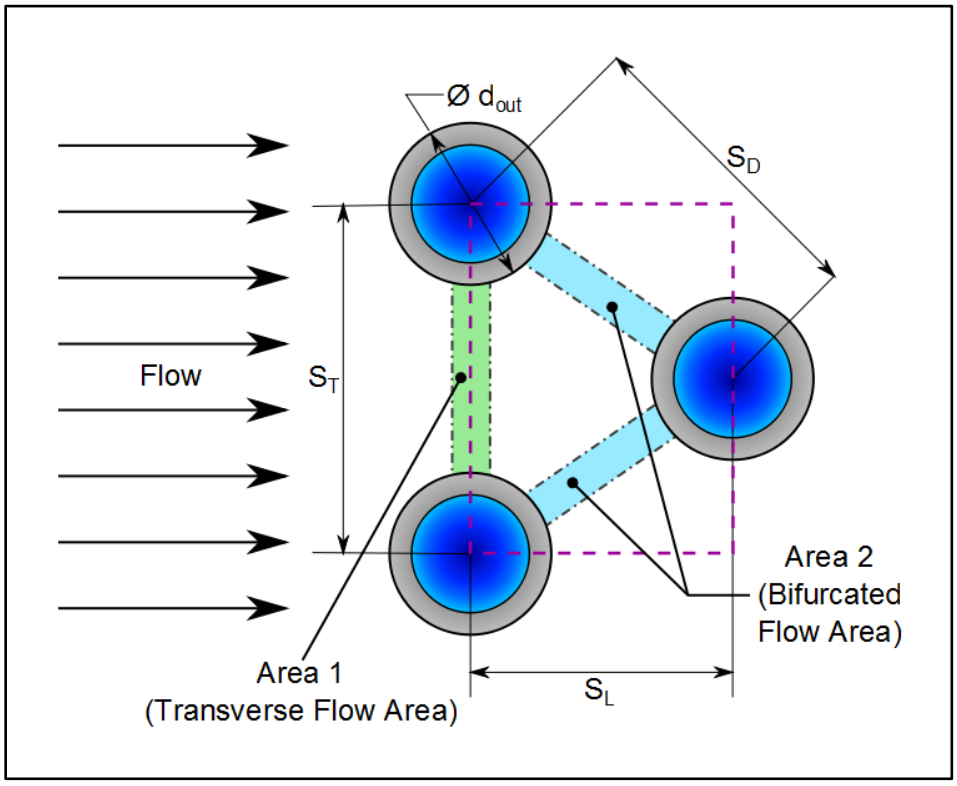

Figure 11 - Staggered Tube Free Body Diagram

The effect of natural convection at low Reynolds numbers was ignored in this study. Zhukauskas shows that the effect of natural convection becomes insignificant for $Re_D \geq 200$[9]. For simplicity, radiation heat transfer is also ignored.

The calculated heat transfer rate may vary widely depending on the value of the thermal resistance. The conditions for the water side heat transfer are well within the bounds of the Dittus-Boelter equation and thus it is assumed that an analytic model based on equation 5 has merit. The thermal resistance calculation of the cylindrical wall is based on the conduction equation directly and is assumed to be exact within the uncertainty of the given dimensions and material properties. The air-side thermal resistances, however, present a wide range of uncertainty given the flow environment. Four heat transfer models are compared to determine the relative error between the calculation and the measured data. These models are used to compute the Nusselt number given the geometry and the air properties. The four heat transfer models used by the program are the Grimison model, a modified Grimison model, a Zhukauskas model, and the Kays & London model.

2.2.1 Grimison Model

The original Grimison model[7][8] for staggered tubes arrangements was developed in 1937. It computes the Nusselt number for a bank of tubes as

$$Nu = 1.13\, C_1 C_2\, Re_{D,max}^{m} Pr^{1/3} \qquad \begin{bmatrix} 2000 < Re_{D,max} < 40{,}000 \\ \Pr \geq 0.7 \end{bmatrix} \tag{13}$$

where C_1 and m are listed in table 1 and C_2 is a correction factor for tube banks having less than ten tubes ($N_L < 10$) as listed in table 2.

Table 1 - Constants of Equation 13 for airflow over a staggered tube bank[7][8]

S_L/d_{out}	S_T/d_{out} = 1.25		1.5		2.0		3.0	
	C_1	m	C_1	m	C_1	m	C_1	m
0.600	—	—	—	—	—	—	0.213	0.636
0.900	—	—	—	—	0.446	0.571	0.401	0.581
1.000	—	—	0.497	0.558	—	—	—	—
1.125	—	—	—	—	0.478	0.565	0.518	0.560
1.250	0.518	0.556	0.505	0.554	0.519	0.556	0.522	0.562
1.500	0.451	0.568	0.460	0.562	0.452	0.568	0.488	0.568
2.000	0.404	0.568	0.416	0.568	0.482	0.556	0.449	0.570
3.000	0.310	0.592	0.356	0.580	0.440	0.562	0.428	0.574

Table 2 - Correction factor C_2 of equation 13 for staggered tubes with $N_L < 10$[7]

N_L	1	2	3	4	5	6	7	8	9
C_2	0.68	0.75	0.83	0.89	0.92	0.95	0.97	0.98	0.99

For implementation in the computer program, the coefficients C_1 and m may be determined by the use of the following curve fits as evaluated in the present study:

$$\alpha_{coeff} = -0.066572\left(S_T/d_{out}\right)^2 + 0.438619\left(S_T/d_{out}\right) - 0.534414$$

$$\beta_{coeff} = 0.447806\left(S_T/d_{out}\right)^2 - 2.867419\left(S_T/d_{out}\right) + 3.482562$$

$$\gamma_{coeff} = -1.046594\left(S_T/d_{out}\right)^2 + 6.359781\left(S_T/d_{out}\right) - 7.686638$$

$$\delta_{coeff} = 0.803673\left(S_T/d_{out}\right)^2 - 4.605252\left(S_T/d_{out}\right) + 5.975412$$

$$\alpha_{exp} = 0.009058\left(S_T/d_{out}\right)^2 - 0.076068\left(S_T/d_{out}\right) + 0.104510$$

$$\beta_{exp} = -0.071578\left(S_T/d_{out}\right)^2 + 0.534418\left(S_T/d_{out}\right) - 0.706706$$

$$\gamma_{exp} = 0.193359\left(S_T/d_{out}\right)^2 - 1.270342\left(S_T/d_{out}\right) + 1.608849$$

$$\delta_{exp} = -0.154482\left(S_T/d_{out}\right)^2 + 0.934097\left(S_T/d_{out}\right) - 0.585832$$

$$C_1 = \alpha_{coeff}\left(S_L/d_{out}\right)^3 + \beta_{coeff}\left(S_L/d_{out}\right)^2 + \gamma_{coeff}\left(S_L/d_{out}\right) + \delta_{coeff}$$

$$m = \alpha_{exp}\left(S_L/d_{out}\right)^3 + \beta_{exp}\left(S_L/d_{out}\right)^2 + \gamma_{exp}\left(S_L/d_{out}\right) + \delta_{exp}$$

These fitted data agree well with the data given from table 1 as shown in figures 12 and 13.

Note that equation 13 relies on the use of

$$Re_{D,max} \equiv \frac{\rho V_{max} d_{out}}{\mu} \tag{14}$$

where

$$V_{max} = \begin{cases} \dfrac{S_T}{S_T - d_{out}} V & for\ S_D \geq \dfrac{S_T + d_{out}}{2} \\ \dfrac{S_T}{2(S_D - d_{out})} V & for\ S_D < \dfrac{S_T + d_{out}}{2} \end{cases} \tag{15}$$

$$S_D \equiv \sqrt{S_L^2 + \left(\frac{S_T}{2}\right)^2}$$

The S_D criterion is used to determine if the maximum velocity occurs in the transverse plane (Area 1 in figure 11) or if the maximum velocity occurs in the

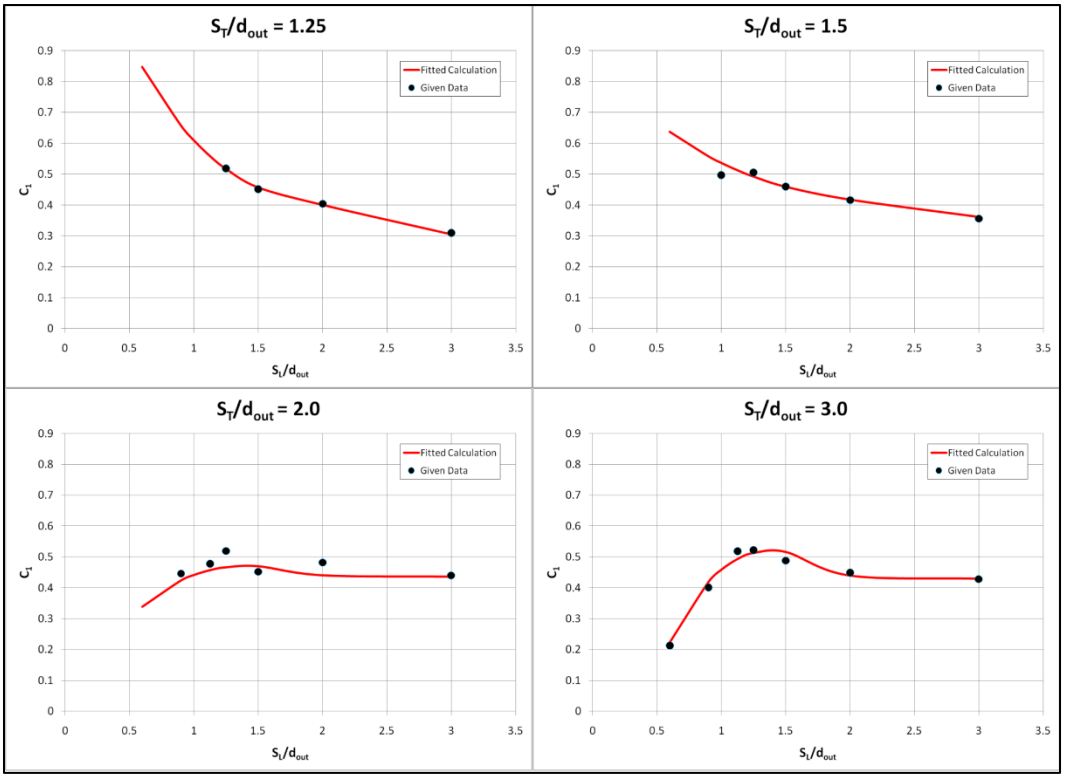

Figure 12 - Comparison of the C_1 Coefficients with Fitted Data

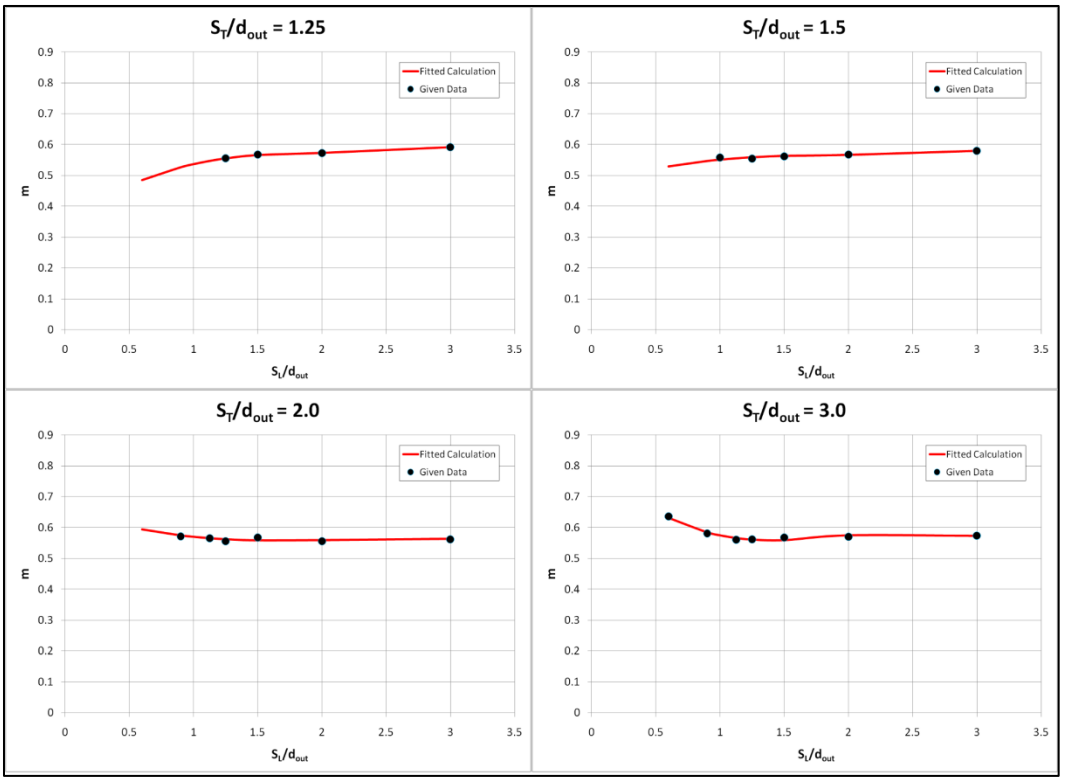

Figure 13 - Comparison of the m Exponents with Fitted Data

diagonal plane when the flow is bifurcated by the staggered tube arrangement (Area 2 in figure 11).

2.2.2 Modified Grimison Model

A few potential problems with the original Grimison model may be noted as relating to higher temperature cross-flows. Because of the higher temperatures on the air side, $Pr < 0.7$; which is outside the domain of the valid Prandtl numbers given in the reference.

Another potential concern is the Reynolds number. For an input air mass flow rate and shell side area the flow velocity was computed as:

$$V = \frac{\dot{m}}{\rho A} = \frac{\dot{m}}{\rho(HW)}$$

For the typical conditions used in H2, the mass flow rate is low enough—and the heat exchanger area is large enough—that the Reynolds number calculated by equation 14 is typically much less than 2000.

Observe that equation 13 is more sensitive to the Reynolds number than the Prandtl number by comparing the magnitudes of the exponents of these two arguments. For all geometries given in table 1, $m > {}^{1}/_{3}$; also, for the cases presented herein, $Re \sim O(100)$ while $\mathrm{Pr} \sim O(1)$. These magnitudes also indicate that the Reynolds number has a larger influence on the relations than the Prandtl number. In order to correct the Grimison equation for the conditions beyond the lower bounds, the present study introduced a coefficient, ξ_H. This coefficient should allow for the specification of $Nu = 0$ for $Re_{D,max} = 0$ and, ideally, gives $\xi_H = 1$ for

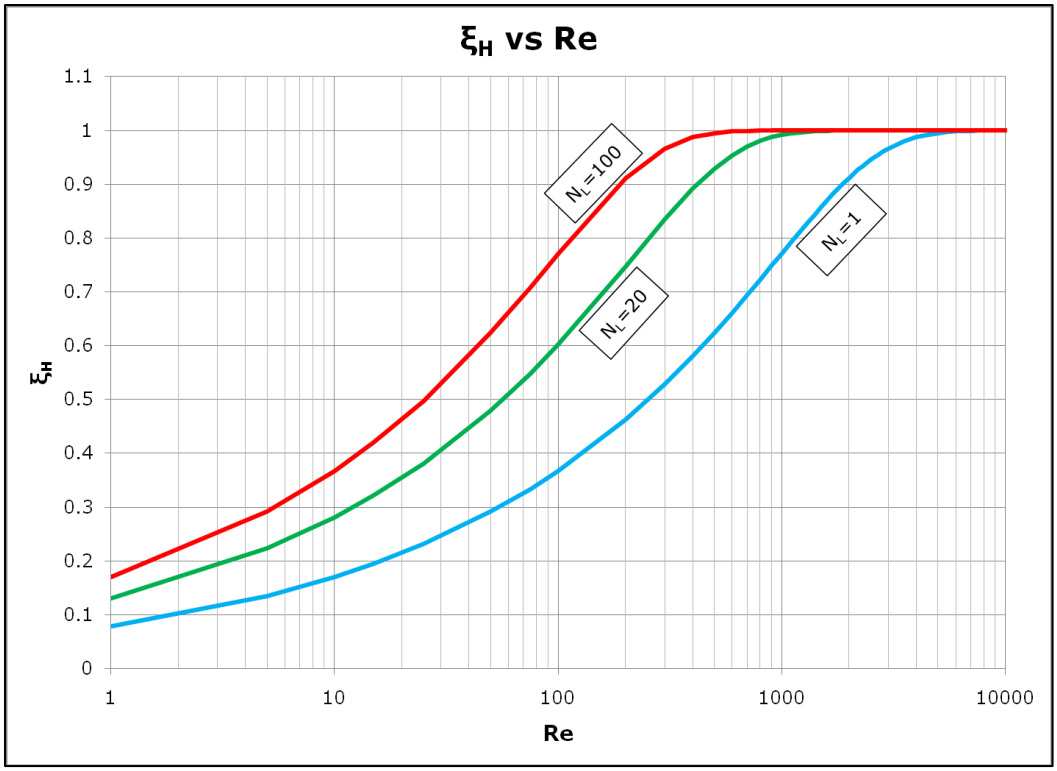

Figure 14 – ξ_H Correction to the Original Grimison Model ($Pr = 0.69$)

$Re_{D,max} = 2000$ and $Pr = 0.71$. For simplicity, consider a function that asymptotically approaches a value of 1 as its parameters increase. The hyperbolic tangent function is one such function and gives a steeper rise than a variant of $1 - e^{-f(Re)}$. Also use the standard temperature and pressure values for air as a reference Pr as well as the reference Reynolds number of 2000. For overall heat transfer analyses, a factor is also needed to account for the number of tube rows in the exchanger, otherwise the values of ξ_H will be too low when analyzing the entire non-discritized heat exchanger. Note that since the numerical model calculates the heat transfer by discrete rows, $N_L = 1$ for each row heat transfer computation. By these criteria, a modified Grimison model may be represented by equations 16 with the correction factor equation 17 as proposed herein. Equation 17 is plotted in figure 14 for

various values of N_L. The coefficients C_1 and C_2 and the exponent m are all referenced from tables 1 and 2 or the previously discussed curve fits.

$$Nu = 1.13\,\xi_H C_1 C_2\, Re_{D,max}^{m} Pr^{1/3} \tag{16}$$

$$\xi_H = \left[\tanh\left\{\sqrt{N_L}\left(\frac{Re_{D,max}}{2000}\right)\left(\frac{Pr}{0.71}\right)^{1/3}\right\}\right]^{1/3} \tag{17}$$

Note that this is a simple alteration to the original Grimison model by solving for one additional scaling factor using the pre-computed Reynolds number and Prandtl number.

2.2.3 Zhukauskas Model

The Zhukauskas model, published in 1972, is given in equation 18[7][9][10]. The model has been used extensively since its publication and is presented in many textbooks on convection heat transfer such as those of Bejan[11] and Incropera & DeWitt[7]. The Zhukauskas model has been reported to be accurate to within ±15%[11].

As can be observed, this model calculates the Nusselt number following the form of equation 1 with a correction for a thermal gradient due to the tube wall temperatures being cool relative to the hot air temperatures.

$$Nu = C_1 C_2\, Re_{D,max}^{m} Pr^{n} \left(\frac{Pr}{Pr_s}\right)^{1/4} \tag{18}$$

$$\begin{bmatrix} 10 < Re_{D,max} < 2 \times 10^6 \\ 0.7 < \mathrm{Pr} < 500 \end{bmatrix}$$

This equation uses $Re_{D,max}$ as calculated using equations 14 and 15. The coefficient C_2 is used to correct the Nusselt number for banks having less than 20 tubes as given in tables 3 (for $Re < 1000$) and 4 (for $Re \geq 1000$).

Table 3 - Correction factor C_2 for staggered tubes with $N_L < 20$[9][11] for $Re < 1000$

N_L	1	2	3	4	5	7	10	13	16
C_2	0.83	0.88	0.91	0.94	0.95	0.97	0.98	0.99	1.0

Table 4 - Correction factor C_2 for staggered tubes with $N_L < 20$[7] for $Re \geq 1000$

N_L	1	2	3	4	5	7	10	13	16
C_2	0.64	0.76	0.84	0.89	0.92	0.95	0.97	0.98	0.99

Note that the data presented in tables 3 and 4 can be numerically approximated by the conditional equation

$$C_2 = \begin{cases} 1 - e^{\left(-N_L^{1/\sqrt{3}}\right)} & Re > 1000 \\ 1 - e^{-\sqrt{3N_L^{1/\sqrt{2}}}} & Re \leq 1000 \end{cases} \tag{19}$$

The coefficient C_1 and the exponents m and n are determined from table 5.

Table 5 - Constants of equation 18 for airflow over a staggered tube bank[7]

$Re_{D,max}$	C_1	m	n
$10 - 100$	0.90	0.40	0.36
$100 - 1000$	Approximate as an isolated cylinder		
$1000 - 2 \times 10^5$ $\left(S_T/S_L\right) < 2$	$0.35\left(S_T/S_L\right)^{0.2}$	0.6	0.36
$1000 - 2 \times 10^5$ $\left(S_T/S_L\right) \geq 2$	0.40	0.6	0.36
$2 \times 10^5 - 2 \times 10^6$	0.022	0.84	0.36

Note that for the condition $100 \leq Re_{D,max} < 1000$ Zhukauskas proposes that the tube bank be approximated by a single, isolated cylinder. For this case, Zhukauskas proposes that the Nusselt number be computed by equation 20 which differs from equation 18 only in that the Reynolds number used is based on the control volume freestream inlet velocity, V, rather than the maximum fluid velocity based on tube area constriction, V_{max} (i.e. $Re_D \equiv \frac{\rho V d_{out}}{\mu}$ is used rather than $Re_{D,max}$).

$$Nu = C_3 C_2 \, Re_D^m Pr^n \left(\frac{Pr}{Pr_s}\right)^{1/4} \tag{20}$$

$$n = \begin{cases} 0.36 & Pr > 10 \\ 0.37 & Pr \leq 10 \end{cases}$$

The coefficient C_3 and the exponent m are given in table 6. Equation 20 also uses the correction factor C_2 as read from tables 3 and 4.

Table 6 - Constants of equation 19 for airflow over a staggered tube bank[7]

Re_D	C_3	m
1—40	0.75	0.4
40—1000	0.51	0.5
10^3—2×10^5	0.26	0.6
2×10^5—10^6	0.076	0.7

Zhukauskas did publish an adjusted model in 1987 where the intervals and coefficients of table 5 were adjusted and the model no longer assumed an isolated cylinder for some flow regimes. When comparing the 1987 model to the 1972 model presented here, the results were little better than the original Grimison

model for the low Reynolds number cases seen by the H2 heat exchanger. So for this analysis the 1972 model, as published in references [7] and [10], was used.

In both equations 18 and 20 the property Pr_s is evaluated using the tube wall temperature. Because the tube wall temperature will not initially be known at the time of the Nusselt number calculation, an initial film Prandtl number must be assumed.

Assume that the tube wall temperatures are typically in the range 100°F—600°F and having ambient air pressure of 1.5 psia. Using equilibrium air calculations, the following Prandtl number data is obtained.

Table 7 - Air Prandtl Number at Typical Tube Wall Temperatures

T	Pr
100°F	0.70
200°F	0.69
400°F	0.67
600°F	0.68

Averaging the data from table 7 produces $Pr_{s,avg} = 0.69$ which, coincidentally, corresponds to a tube wall temperature of approximately 200°F. Because for most cases presented, the tube wall will be less than 200°F and this average Prandtl number value will be an acceptable approximation.

To prove this statement, the effect of the $\left({}^{Pr}/_{Pr_s}\right)^{1/4}$ term was examined:

Table 8 - Zhukauskas Equation Prandtl Number Relative Error Considerations

Pr_s	${}^{Pr}/_{Pr_s}$	$\left({}^{Pr}/_{Pr_s}\right)^{1/4}$
0.70	$(1.43)Pr$	$(1.09)Pr^{0.25}$
0.69	$(1.45)Pr$	$(1.10)Pr^{0.25}$
0.67	$(1.49)Pr$	$(1.11)Pr^{0.25}$
0.68	$(1.47)Pr$	$(1.10)Pr^{0.25}$

The absolute error of this is $1.11Pr^{0.25} - 1.09Pr^{0.25} = 0.02Pr^{0.25}$ and the relative error of the spread is 1.8%. Using a $Pr_{s,avg}$ of 0.69 has a calculation error of 1.4% to 1.5% for $T_{wall} = 100°\text{F}$ and $T_{wall} = 600°\text{F}$, respectively.

It should be noted that iterating the heat transfer equation based on a feedback loop incorporating the Nusselt number and the tube wall temperature until a convergence criterion is reached would improve the fidelity of the model.

2.2.4 Kays & London Model

The Kays & London model was introduced in 1984 to calculate the *overall* heat exchanger performance of so-called compact heat exchangers[12]. The authors recommended the use of the Colburn j factor as shown in equation 21 using the Stanton number, St, and the Prandtl number to compute the heat transfer of gas flow normal to an *infinite* bank of tubes.

$$j_H = StPr^{2/3} = {h}/{Gc_p}\, Pr^{2/3} \tag{21}$$

Rearranging equation 21 to solve for the convective heat transfer coefficient gives

$$h = j_H \frac{Gc_p}{Pr^{2/3}} \tag{22}$$

Recognizing that $Nu \equiv \frac{hd_{out}}{k}$ and $Re = \frac{Gd_{out}}{\mu}$ (for cylindrical tubes), the Nusselt number may be expressed as:

$$Nu_\infty = j_H \mu c_p k^{-1} RePr^{-2/3} \tag{23}$$

Recall that $Pr \equiv \frac{\mu c_p}{k}$. Using this definition, the previous relation simplifies to yield

$$Nu_\infty = j_H Re Pr^{1/3} \tag{24}$$

In their book *Compact Heat Exchangers*, Kays & London[12] present the relation

$$j_H = C_h Re^{-0.4} \quad \text{for } 300 < Re < 15{,}000 \tag{25}$$

where the term C_h is a function of $\left(\frac{S_T}{d_{out}}\right)$ and $\left(\frac{S_L}{d_{out}}\right)$ and (for the geometries given) is bounded by $0.2 \leq C_h \leq 0.425$.

Observe that substituting equation 25 into equation 24 yields equation 26. Comparing equation 26 with equation 13 from the range of scalar coefficients from table 1 will show that the Kays & London heat transfer relation very closely resembles the Grimison heat transfer model; however, the coefficients used by the Kays & London model are meant for "compact" heat exchanger geometries ("compact" meaning $1.5 \leq \frac{S_T}{d_{out}} \leq 2.5$ and $0.75 \leq \frac{S_L}{d_{out}} \leq 1.5$). Notice that equation 26 mirrors equation 1 where $m = 0.6$ and $n = {}^1/_3$.

$$Nu_\infty = C_H Re^{0.6} Pr^{1/3} \tag{26}$$

Recall that equation 21 was developed with the assumption of an *infinite* bank of tubes. This is corrected by applying (as similar to both the Grimison and the Zhukauskas models) the relation:

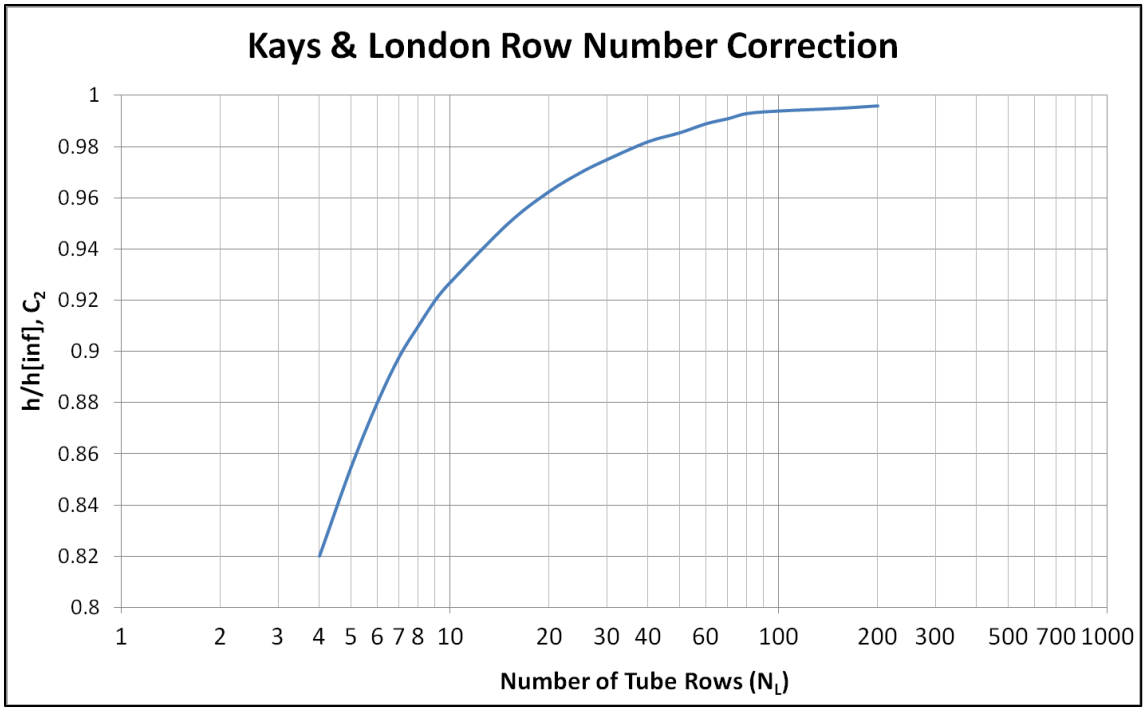

Figure 15 - Kays & London influence of N_L variations in the heat transfer coefficient[12]

$$Nu = C_2 Nu_\infty \tag{27}$$

Kays & London presented (graphically) a correction for finite tube banks duplicated in figure 15. The scaling may numerically be approximated using the equation:

$$C_2 \approx \frac{N_L^{0.728} + 1}{N_L^{0.72}} - \frac{N_L^{-0.2}}{\ln(N_L)} \tag{28}$$

2.2.5 First Law Analysis

The heat transfer rate through the air cooler may be quantified using the first law of thermodynamics. The first law being defined as

$$\dot{q} - \dot{w} = \dot{m}_{air}\left\{\left(i_{air,inlet} + \frac{{V_{inlet}}^2}{2} + gZ_{inlet}\right) - \left(i_{air,outlet} + \frac{{V_{outlet}}^2}{2} + gZ_{outlet}\right)\right\} \quad (29)$$

Assuming that the potential energy of the system is negligible, the kinetic energy terms are much less than the enthalpy terms ($\frac{V^2}{2} \ll i_{air}$, $\frac{V^2}{2} \sim 0.1\ {}^{Btu}/_{lb_m}$), and that there is no component in the system to produce work, equation 29 reduces to

$$\dot{q} = \dot{m}_{air}\left(i_{air,inlet} - i_{air,outlet}\right) \quad (30)$$

2.2.6 Heat Exchanger Effectiveness

A common method of heat exchanger analysis is to determine the *effectiveness* of the exchanger. The heat exchanger effectiveness is defined as

$$\varepsilon \equiv \frac{\dot{q}}{\dot{q}_{max}} \quad (31)$$

where $\dot{q}_{max}$ is the maximum possible heat transfer amount of the system in which the outlet temperature of the air (the hot fluid) is equal to the inlet temperature of the water (the cold fluid). As such, the maximum possible heat transfer rate may be defined as such:

$$\dot{q}_{max} = \dot{m}_{air}\left\{i_{air,inlet} - i_{air}\left(T_{water,inlet}\right)\right\} \quad (32)$$

Therefore, the effectiveness of the exchanger may be represented in terms of the inlet and outlet enthalpies of the exchanger in addition to the enthalpy of air at the inlet temperature of the cooling fluid.

$$\varepsilon \equiv \frac{\dot{q}}{\dot{q}_{max}} = \frac{i_{air,inlet} - i_{air,outlet}}{i_{air,inlet} - i_{air}\left(T_{water,inlet}\right)} \tag{33}$$

Note that in the case where the outlet air temperature is equal to the inlet water temperature, the effectiveness will be equal to unity.

2.3 Pressure Drop Models

There are several models available that may be adopted to calculate the pressure drop across a bank of staggered tubes. In most models, the pressure drop is a function of the flow velocity, flow density, geometry conditions, and a scalar friction factor value that depends on the parameters of the tubes as well as the Reynolds number of the flow.

2.3.1 Holman-Jakob Model

The Holman-Jakob model[13], introduced in 1938, relates the pressure drop across a bank of tubes by the relation:

$$\Delta p = \frac{G_{max}^2 N_L}{\rho\left({}^{g}/_{2}\right)}\left(\frac{\mu_w}{\mu}\right)^{0.14}\left[0.25 + \frac{0.118}{\left(\frac{S_T - d_{out}}{d_{out}}\right)^{1.08}}\right] Re_{D,max}^{-0.16} \tag{34}$$

(English units only, $[\Delta p] = {}^{lb_f}/_{ft^2}$)

Note that equation 34 has no arguments to account for variations in tube material and thus the model would under predict the pressure drop for rough tubes while potentially over predicting the pressure drop for idealistically smooth tubes.

2.3.2 Gunter-Shaw Model

The Gunter-Shaw model[14] was published in 1945 and implements a piecewise friction factor correction based on the Reynolds number of the flow. Gunter and Shaw present the following friction relation[14]

$$\frac{f}{2} = \frac{\Delta p g D_v \rho}{G^2 \ell} \left(\frac{\mu}{\mu_w}\right)^{0.14} \left(\frac{D_v}{S_T}\right)^{-0.4} \left(\frac{S_L}{S_T}\right)^{-0.6} \tag{35}$$

Solving this relation in terms of the pressure drop yields the Gunter-Shaw pressure drop relation

$$\Delta p = \frac{f}{2} \frac{1}{g} \left(\frac{\mu_w}{\mu}\right)^{0.14} \left(\frac{D_v}{S_T}\right)^{0.4} \left(\frac{S_L}{S_T}\right)^{0.6} \left\{\frac{G^2 \ell}{D_v \rho}\right\} \tag{36}$$

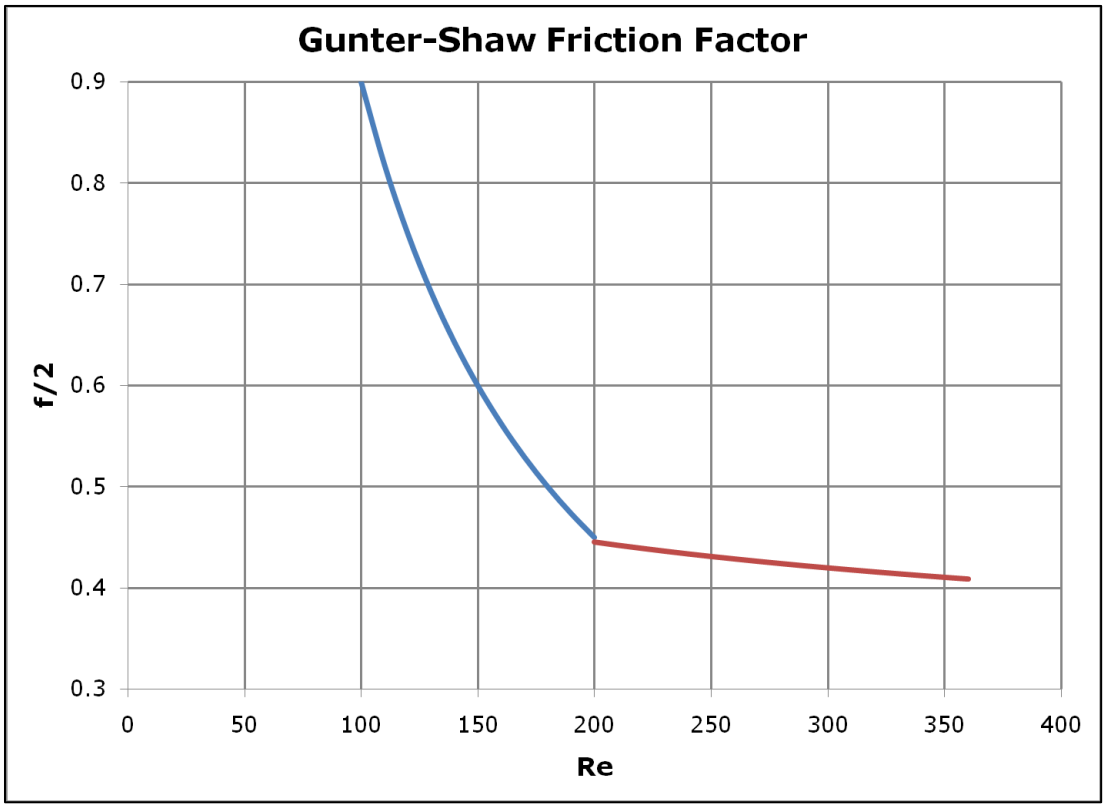

Figure 16 - Gunter-Shaw Crossflow Friction Factors

Gunter and Shaw assume a laminar-to-turbulent transition point at $Re \cong 200$. By their correlations, they present a piecewise friction factor relation of the form[14]:

$$\frac{f}{2} = \begin{cases} 90\, Re^{-1} & for\ Re \leq 200 \\ 0.96\, Re^{-0.145} & for\ Re > 200 \end{cases} \tag{37}$$

Notice that the values of both functions in equation 37 are equal at $Re \cong 202.488$.

Note that for the case of a staggered tube arrangement, the volumetric hydraulic diameter used in equation 36 may be expressed in terms of the heat exchanger's given dimensions as:

$$D_v \equiv \frac{4 \times (Net\ Free\ Volume)}{(Friction\ Surface)} = \frac{4 \times \left(S_T S_L - \frac{\pi}{4} d_{out}^2\right)}{\pi d_{out}}$$

$$D_v = \frac{4}{\pi} \frac{S_T S_L}{d_{out}} - d_{out} \tag{38}$$

2.3.3 Boucher and Lapple's Correction to the Gunter-Shaw Model

In 1945, Boucher and Lapple[14] critiqued the Gunter-Shaw model by stating that the friction factors given by Gunter and Shaw are fairly good over a small range of configurations, but "become progressively worse as more extreme spacings are approached"[14].

These authors continue their discussion of the Gunter-Shaw model and state that:

> [The Gunter-Shaw] method of correlation does give a good representation of the data in the range of spacings commonly employed, but will yield low values for wide spacings.[15]

It will be shown that this comment by Boucher and Lapple appears to be correct. The present study found that the Gunter-Shaw model regularly underpredicts the pressure drop for the H2 cooler.

For the geometries present in the H2 cross flow heat exchanger, the friction factors calculated by equation 37 are too low and are thus corrected by multiplying by the scalar value of 1.75 to increase effect of the viscous losses. This factor was determined in the present study as Boucher and Lapple do not give an explicit correction to the Gunter-Shaw model, but they do specify that the friction factors as calculated by Gunter and Shaw give unduly low results at wide transverse spacings[15].

2.3.4 Zhukauskas Model

The Zhukauskas pressure drop model was included in Zhukauskas's work on an improved heat transfer model for crossflow tube banks. The Zhukauskas model is expressed as[10][11]

$$\Delta p = N_L \mathcal{X} \left(\frac{\rho V_{max}^2}{2} \right) f \tag{39}$$

where the friction factor f and the correction factor $\mathcal{X}$ are presented graphically for staggered tube banks.

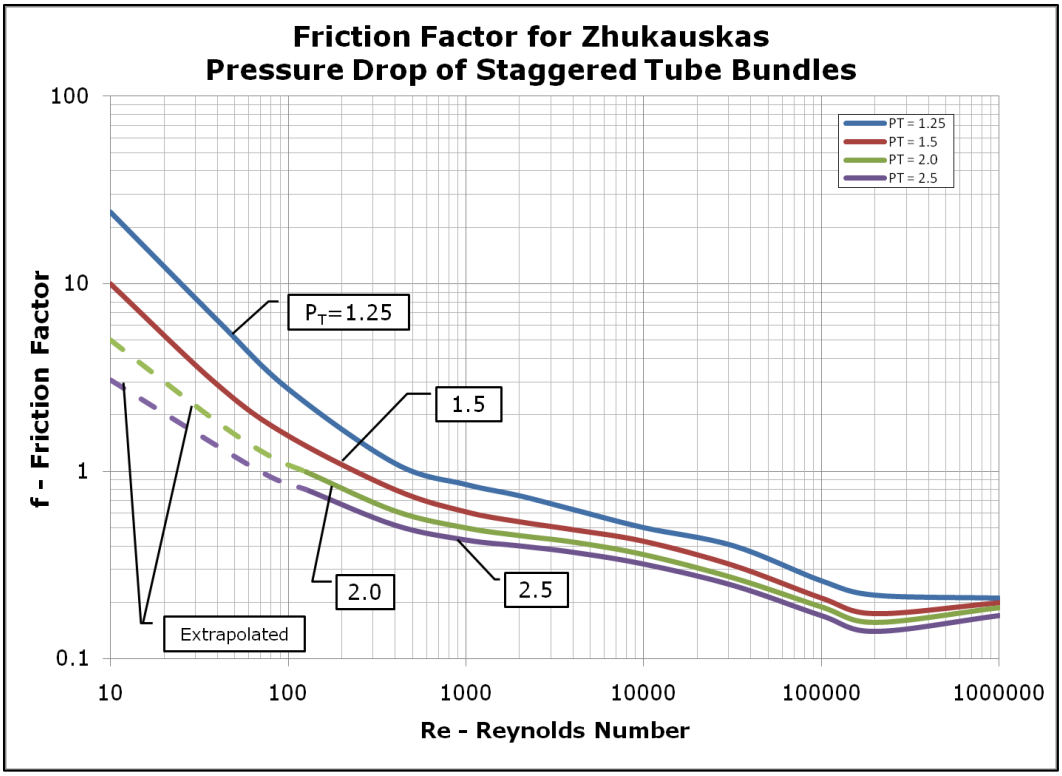

Figure 17 - Friction Factor for Zhukauskas Pressure Drop Model (Equation 39)

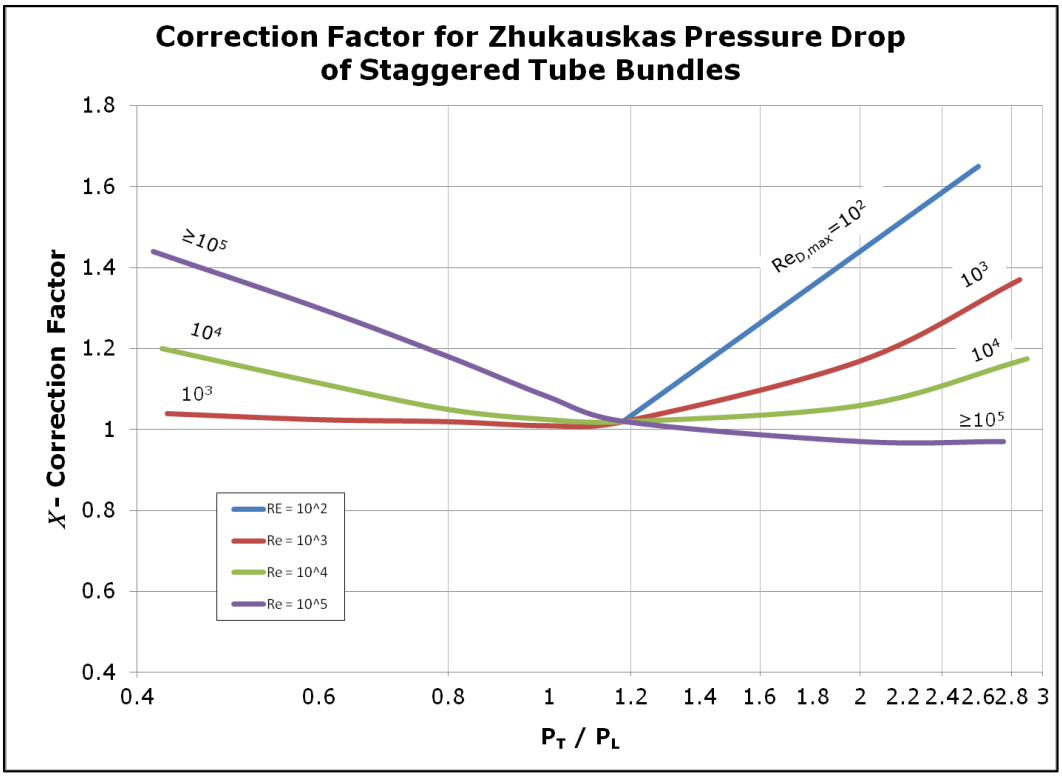

Figure 18 - Geometry Correction Factor for Zhukauskas Pressure Drop Model

These plots are reproduced using cubic splines in figures 17 and 18. Note that the data in figures 17 and 18 are presented in terms of dimensionless longitudinal and transverse pitches, $P_L \equiv S_L/d_{out}$ and $P_T \equiv S_T/d_{out}$. The cubic spline coefficients that reproduce the curves shown in figures 17 and 18 are presented in Appendices B and C.

For the numerical model, the friction factor is logarithmically interpolated between the geometry curves. It is for this reason that the $P_T = 2.0$ and $P_T = 2.5$ curves are extrapolated into the low Reynolds number regime. This allows the $P_T = 2.0$ and $P_T = 2.5$ curves to have the same calculation domain as the $P_T = 1.25$ and $P_T = 1.5$ curves. The correction factor is linearly interpolated between the Reynolds number order of magnitude curves using the calculated Reynolds number at the correct geometry ratio.

2.3.5 Kays & London Model

The Kays & London pressure drop model was included in the 1984 publication *Compact Heat Exchangers* along with the heat transfer model. In this book, the following pressure drop relation[12] is proposed:

$$\frac{\Delta p}{p_1} = \frac{G^2}{2g_c}\frac{v_1}{p_1}\left[(1+\sigma^2)\left(\frac{v_2}{v_1}-1\right) + f\frac{A}{A_{min}}\frac{v_m}{v_1}\right] \tag{40}$$

where the subscripts 1 and 2 refer to the heat exchanger inlet and outlet, respectively, and $A = A_{surf,o}$. Equation 40 is a much improved form of the pressure drop model that Grimison suggested in reference [8]. Unlike Grimison's pressure

drop model, the Kays & London variant includes terms for tube arrangement spacing. Equation 40 can be rearranged by recognizing that $v = 1/\rho$ and simplify as

$$\Delta p = \frac{G^2}{2g_c\rho_1}\left[(1+\sigma^2)\left(\frac{\rho_1}{\rho_2}-1\right)+f\frac{A}{A_{min}}\frac{\rho_1}{\rho_m}\right] \tag{41}$$

As discussed in the analytic model, the heat exchanger is numerically evaluated on a discretized row-by-row basis. With this discretization, use the control volume shown by figure 19, allowing that the aforementioned subscripts 1 and 2 now refer to the tube row inlet and outlet, respectively. Using this discretization, it can be assumed that the air-side density change over a *single* row of tubes is negligible. Under this assumption, allow $\rho_1 = \rho_2 = \rho$ in which case equation 41 reduces to

$$\Delta p = \frac{G^2 f}{2g_c\rho}\frac{A_{surf,o}}{A_{min}} \tag{42}$$

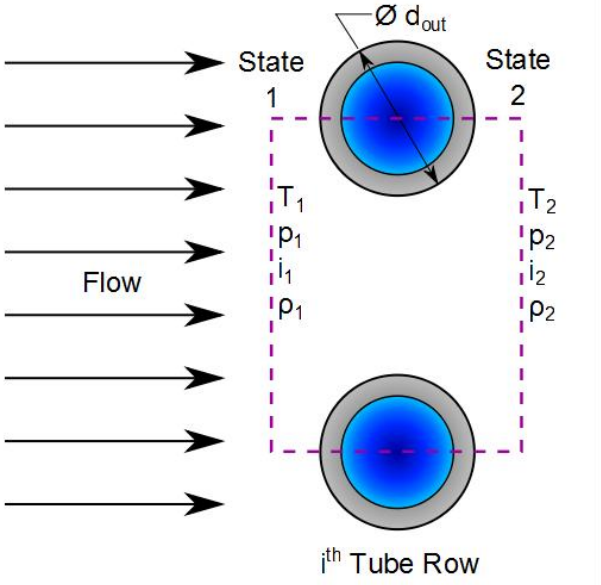

Figure 19 - Control Volume of a Single Tube Row

Kays and London specified a relation for determining the value of the friction factor f as a power law function of the Reynolds number given by the equation

$$f = C_f Re^{-0.18} \tag{43}$$

where the scalar term C_f is a function of $\left(\frac{S_T}{d_{out}}\right)$ and $\left(\frac{S_L}{d_{out}}\right)$ and (for the geometries given) is bounded by $0.15 \leq C_f \leq 0.452$.

The next difficulty is in the determination of the *minimum* free flow area, A_{min}. Refer to the areas given previously in figure 11. Assuming a unit length, recognize that the free flow area in the transverse plane is given by

$$A_{trans} = S_T - d_{out} \tag{44}$$

In the case of the bifurcated flow area, recognize that the diagonal pitch may be expressed as

$$S_D = \sqrt{S_L^2 + \left(\frac{S_T}{2}\right)^2} \tag{45}$$

Subtracting the diameter from the above equation to get the linear distance between diagonal tube walls and recalling that there are two interspacial areas gives the bifurcated flow area equation (again assuming unit length)

$$A_{bif} = 2\left[\sqrt{S_L^2 + \left(\frac{S_T}{2}\right)^2} - d_{out}\right] \tag{46}$$

Now, the minimum free flow area may be expressed by the conditional equation

$$A_{min} = \min\left\{S_T - d_{out}\ ,\ 2\left[\sqrt{S_L^2 + \left(\frac{S_T}{2}\right)^2} - d_{out}\right]\right\} \tag{47}$$